The Cryosphere Discuss., 7, 5659–5682, 2013
www.the-cryosphere-discuss.net/7/5659/2013/
doi:10.5194/tcd-7-5659-2013

The Cryosphere
Discussions
Open Access

Review article: the false–bottom ice

D. V. Alexandrov[1], **J. Jouzel**[2], **I. Nizovtseva**[1,2], **and L. B. Ryashko**[1]

[1]Ural Federal University, Ekaterinburg, Russian Federation
[2]Laboratoire des Sciences du Climat et de l'Environnement/Institut Pierre Simon Laplace (LSCE/IPSL CEA), France

Received: 28 September 2013 – Accepted: 8 November 2013 – Published: 21 November 2013

Correspondence to: J. Jouzel (jean.jouzel@lsce.ipsl.fr)

Published by Copernicus Publications on behalf of the European Geosciences Union.

Abstract

Nansen from his observations in the Beaufort Sea published in 1897 noted that heat transfer from the fresh water (with a temperature of 0 °C) to the arctic salt water (with a temperature of −1.6 °C) is the only source of ice accretion during the polar summer. This transfer mechanism, unusual at first sight, is responsible for the initiation and evolution of a false bottom ice, changing ice properties to a great extent and affecting various processes while interacting with the ocean and the atmosphere. The processes of false bottom ice growth from below (i.e. from the ocean to the atmosphere) become of prime importance in the era of global warming and climate change. In this review, we summarize the theoretical approaches, field and laboratory observations, conducted during more than 100 yr, in order to address the problem of false bottoms to a broad community of readers. We also discuss the recent modeling advances to which we have contributed. A "false bottom" is a thin layer of ice which forms in summer underneath the floe, where fresh water lies between the salt water and the ice. Such false bottoms represent the only significant source of ice growth in the Arctic during the spring-summer period. Their evolution influences the mass balance of the Arctic sea-ice cover, which is recognized as an indicator of climate change. However, the quantity, aerial extent and other properties of false bottoms are difficult to measure because coring under the surface melt ponds leads to direct mixing of surface and under-ice water. This explains why their aerial extent and overall volume is still not known despite the fact that the upper limit of the present-day estimate of the false bottom ice coverage is approximately half of the sea ice surface. The growth of false bottoms also leads to other important consequences for various physical, chemical and biological processes associated with their dynamics.

1 Introduction

The thermodynamics and interactions of ice masses with the ocean and atmosphere represent a central theme in glaciological studies. The polar expeditions at the end of the 19th century, described by Nansen (1897) and Stefan (1889), put forward a number of important scientific issues related to the ice freezing processes and their influence on the heat exchange between the ocean and the Earth's atmosphere. The heat exchange processes play an important role in the air mass motion and influence on the weather conditions formation, as shown by Ackley (1979), Randall et al. (1998), Budikova (2009). In order to take into account the influence of these processes on the atmospheric dynamics, it is necessary to quantify the heat flux released into the atmosphere.

In the nineties Peixoto and Oort (1992) have shown that approximately half of the surface heat flux can be connected with the latent heat of crystallization. A significant part of this flux is related to the freezing of seawater in the newly formed ice cracks that form due to the mechanical stress in the ice cover. For example, the heat flux going to the atmosphere from these cracks is about 300 W m^{-2}, which is approximately 15 times greater than the flux from the surface of the surrounding ice (The LeadEx Group, 1993). In the spring–summer period, when the air temperature is above 0 °C, weather conditions cause ablation to occur. As a result, a considerable fraction of meltwater concentrated in puddles at the ice surface penetrates through the ice matrix beneath the lower ice boundary, accumulates in bottom depressions and forms fresh water lenses or under-ice melt ponds (Hanson, 1965).

Thus, a supercooled (transition) layer appears in the region where the fresh water comes into a contact with the salt water. As a result, at the upper edge of this transition layer, a zone of supercooled and lightest water arises. Since the density of salt water (with salinity less than 23 ‰ and within the temperature interval $-1 \le T \le 1\,^{\circ}$C) decreases with supercooling (see Figs. 7 and 8 presented by Martin and Kauffman, 1974), the upper edge of water in this transition region is convectively unstable. Mean-while, as the density decrease caused by the temperature change from 0 to −1 °C compensates the density increase caused by a salinity increase, supercooling produces a density inversion only for very small salinities (Martin and Kauffman, 1974). As a result, ice crystals appear at nucleation sites within this upper edge of supercooled transition layer. The effect of density inversion leads to the fact that the ice crystals float within this transition layer and grow in downward direction where the salt water is colder. Martin and Kauffman (1974) in their pioneering experiments demonstrated that the growing crystals were randomly oriented in a horizontal plane with a spacing of order 1 cm, so that the different vertical ice sheets interlocked and formed a stable downward-growing crystal matrix. After a lapse of time, the downward growth rate of the ice crystals decreases and most of the new ice occasionally grows laterally until a horizontal ice sheet forms.

This underwater ice is called the “False Bottom” by Untersteiner and Badgley (1958), Cherepanov et al. (1989), Eicken (1994), Eicken et al. (2002), Perovich et al. (2003), Polashenski et al. (2011) (we illustrate false bottoms in Figs. 1 and 2). Manuscripts by Martin and Kauffman (1975), Eicken (1994) and Perovich et al. (2003) are now considered to provide the classical interpretation of the subject.

In nature, the false-bottom effect occurs under the polar pack ice and at the bottom of ice shelves during the arctic summer according to Martin and Kauffman (1974) and Lyons et al. (1951). When this underwater ice sheet or false bottom forms, it migrates upwards due to bottom ablation (Hanson, 1965; Martin and Kauffman, 1974; Alexandrov and Nizovtseva, 2008a). The process of false bottom formation and evolution dynamics is described in details in Sect. 3 and visualized in the Supplement on http://www.the-cryosphere.net/. Recent studies (e.g., Eicken et al., 2002; Notz et al., 2003; Alexandrov and Nizovtseva, 2008b) confirm that the false bottom could be formed in natural conditions in a few hours and spread laterally up to a few meters. Its thickness can reach a few decimeters, and the growth rate can be as high as a few centimeters per day (Eicken et al., 2002; Notz et al., 2003). Sometimes false bottom formation occurs under cracks and small leads (Notz et al., 2003). The upper limit of the present day estimate of the false bottom ice coverage is approximately half of the sea ice surface (Hanson, 1965).

2 Implications for sea ice and its interactions with the ocean and atmosphere

The evolution of false bottom greatly changes various physical, chemical and biological aspects of the ocean – sea ice – atmosphere interactions. The most relevant are as follows:

1. The existence of false bottom strongly decreases the melting rate of a thin ice cover and its reflectance (Notz et al., 2003; Perovich et al., 2003). The heat flux caused by the growing false bottom makes a significant contribution to the heat exchange processes between the ocean and atmosphere (Notz et al., 2003; Alexandrov and Malygin, 2011; Alexandrov and Nizovtseva, 2008b). Thus, generally speaking, the assumption that thin ice melts more rapidly than thick ice is not valid a priori. The trapped water above false bottom has the highest percentage of meteoric water (i.e., snow meltwater) among all meltwater reservoirs (Eicken et al., 2002). The heat transfer from the trapped meltwater, with a temperature of 0 °C, to the arctic sea water, with a negative temperature (e.g. −1.6 °C), is the only source of ice accretion during the polar summer: Nansen (1897) was the first one to mention this fact.

2. The salinity distribution during the development of the false bottom has at first seemingly C-shaped distribution as shown by Eicken (1994) in his Fig. 5, and by Alexandrov and Malygin (2011). The sea ice grown in false bottom locations differs from ordinary multiyear ice by its thermal conductivity, diffusivity, density, strength and optical transmissivity (Eicken, 1994). The freezing process in the presence of false bottoms is fundamentally different from the process without double diffusion under the ice cover due to the fact that solidification occurs with a phase transition layer, (Martin and Kauffman, 1974; Alexandrov and Malygin, 2011; Alexandrov

and Nizovtseva, 2008b). The supercooled water in such a layer is responsible for the frazil ice formation (Steele et al., 1989; McPhee, 2008).

3. The process of false bottom migration can be responsible for the structural transitions from the columnar type to the columnar/granular type of the sea ice structure (see discussions presented by Alexandrov and Malygin, 2011). The low permeability of the false bottoms ice covers is responsible for the formation of ice blisters and bulges when pressure builds up upon freezing in the freshwater cavities above false bottoms (Eicken, 1994; Wadhams, 1988; Wadhams and Martin, 1990). False bottoms may significantly change the ice-albedo feedback by shielding thin ice from the oceanic heat flux and bottom melting (Eicken et al., 2002; McPhee, 2008). The structure and form of underwater ice cover are associated with the phase transition processes in false bottoms both experimentally and theoretically. These studies are represented in a number of papers (see, among others, Martin and Kauffman, 1974; Alexandrov and Nizovtseva, 2008b; Alexandrov and Malygin, 2011). The δ^{18}O anomalies observed in Arctic sea ice can be explained by under-ice pond freeze-up in winter (Eicken, 1994).

4. The entrainment of sediments through the ice changes the surface energy balance of the ice cover and significantly reduces the fluxes of shortwave radiation into the underlying water due to the sensitivity of ice optical properties to even small concentrations of opaque impurities as shown by Light et al. (1998) and Eicken et al. (2005). Both the transport processes of meltwater through the ice and its accumulation under ice cover play an important role in the transfer of pollutants and biological organisms therein with their possible further freezing owing to the growth of the false bottom (Gradinger, 1996). In Arctic sea ice these processes of the false bottom growth give an additional contribution to the biomass concentration in the lower centimeters of the ice cover (Spindler, 1990). Biological organisms concentrated in the interstices between the ice platelets of a mushy layer (Jeffries et al., 1995) and active at temperatures down to −20 °C (Junge

et al., 2004) confirm the concept that liquid inclusions in false bottoms provide an adequate habitat for microbial populations on Earth and possibly elsewhere. Under-ice ponds and false bottoms represent a potential site of significant sediment runoff; trapped biological organisms and pollutants can be released in many cases on complete melting of ice floes (e.g. in the Fram Straight region representing the major outlet of the Arctic Basin), as shown in Eicken (1994) and Pfirman et al. (1990).

Thus, the rapid growth of false bottoms and their wide areal coverage in the Arctic during summer determine the important role of underwater ice evolution on the ocean–sea ice–atmosphere interactions.

3 Origin and evolution of the false bottoms

During the ARCTIC 91 cruise onboard the German research icebreaker “Polarstern” the false bottoms were studied in the central Arctic in late summer as part of an extensive ice-coring program. Eight ice samples out of a total of 52 collected for measurements in different locations contained a false bottom. This gives an estimate of approximately 5 % coverage of the ice by false bottoms assuming that the mean age of the ice is three years (Eicken, 1994). As described by Jeffries et al. (1995), traces of false bottoms were found in 22 samples out of a total of 57 investigated in the Beaufort Sea. This gives an estimate of approximately 10 % coverage of the ice by the false bottoms assuming that the age of the ice is four years. The field experiment SHEBA (Surface Heat Budget of the Arctic Ocean) shows that approximately 15 % of a total of more than 100 mass-balance gauges in the Northern Chukchi Sea developed false bottoms (Perovich, 1999). The false bottoms covered approximately one-half the floe bottom under US drifting station Charlie (Hanson, 1965). According to the available information, this estimate is the upper limit of local ice coverage by the false bottom. In the SHEBA experiments, the formation of multiple layers of the false bottom one below the other was found in individual places (Notz et al., 2003). The aforementioned field observations demonstrate that the false bottoms may be more common than had been previously appreciated.

The process of false bottom initiation and upward migration due to bottom ablation was studied in laboratory experiments by Martin and Kauffman (1974). The first stage of this process after meltwater has penetrated under the ice pack, represents itself its accumulation under the ice cover and the initial convection: supercooled water formed at the fresh/sea water interface rises upwards where nucleation occurs, as the freshwater layer is convectively unstable (Buyevich et al., 2001; Weeks, 2010). In other words, because the density of water with a salinity of < 24.7 psu decreases on cooling, a layer of water forms at the fresh/saline water interface that is both supercooled (because of double diffusion processes, heat diffusing faster than the salt diffusion) and less dense than the overlying water (Weeks, 2010). This leads to unstable vertical density distribution responsible for the free convection. As a result, this supercooled water rises and its solute impurities representing the nucleation sites lead to the formation of thin vertical interlocking ice crystals growing down towards the heat sink. Once ice crystals are nucleated at the freshwater–seawater interface they grow laterally releasing the latent heat and compensating the supercooling (the form of growing ice crystals is shown in Fig. 2, panels d and e). Initiated at the lateral walls of ice cavities and solute impurities this lateral growth leads to the formation of a horizontal ice sheet known as a false bottom. The heat released by ice formation at the top of the false bottom ice sheet goes downward toward the underlying cold seawater. This temperature gradient is responsible for the crystallization process at the upper boundary. Its upward migration accompanied by the effect of salt displacement by the growing ice leads to the formation of constitutional supercooling (Buyevich et al., 2001), which arises in the layer above this boundary at a certain time when the salinity gradient (multiplied by the liquidus slope) exceeds the temperature one. This supercooling leads to the formation of a two-phase (mushy) layer, which migrates upwards and increases in thickness. The lower boundary between the false bottom and the ocean warms due to the aforementioned heat flux and dissolves thereby cooling and diluting the adjacent water back to its freezing point. As a result, the lower boundary moves upwards due to the effect of bottom ablation. Note that, as a rule, the upper boundary moves faster than the lower one. Thus, the process of false bottom initiation has three different stages: (1) the initial convection leading to nucleation and vertical crystal growth down; (2) the lateral growth of vertical crystals at the freshwater – seawater interface responsible for the false bottom formation; and (3) the subsequent upward migration of this horizontal ice sheet representing a mushy layer. This process is shown as a qualitative animation in the Supplement http://www.the-cryosphere.net/ (see also Fig. 1).

The crystal shape of particles composing the underwater ice sheet (Fig. 2) was analyzed in laboratory experiments by Martin and Kauffman (1974): after a lapse of time (except the very initial stage of the process) the crystal shape can be approximated as $x = c_1(\mathrm{erf}(c_2 y) - \mathrm{erf}(c_3 y))$, where c_1, c_2, c_3 are known constants and $\mathrm{erf}(y)$ is the error function. According to laboratory experiments these ice crystals form a thin veneer of ice in the supercooled interior on day 14 after the experiment began. In nature, this process usually only takes a couple of hours. Its speed is high enough to trap Arctic cod within the ice cover (Notz et al., 2003). As was reported by Hanson (1965), a more typical estimate for the upward migration rate of false bottoms is of the order of 1 cm day^{-1}. The first attempt to describe the false bottom growth leans upon the theory of a planar solid–liquid interface (Notz et al., 2003). However, experimental observations show that freezing creates a solid sheet of ice of thickness 2–10 cm at the interface between the fresh and salt water and that loosely packed ice crystals fill the fresh water in the space between the bottom of the pack ice and up to the top of the false bottom ice sheet (Hanson, 1965; Untersteiner and Badgley, 1958; Zubov, 1945; Martin and Kauffman, 1974). These experiments confirm a hypothesis that the false bottom represents a phase transition or mushy layer filled with a supercooled water and ice crystals. This is also confirmed by direct diver's observations: thin vertical crystals ran from the bottom of the pack ice to the top of the ice sheet (Martin and Kauffman,1974). Therefore, the freezing process of upward migration of false bottoms should be studied on the basis of a mushy layer theory.

Generally speaking, crystallization processes leading to false bottom formation below the pack ice cover and under-ice melt ponds or in cracks can be characterized by two phase transition domains (mushy layers), which characterize different freezing regimes (Fig. 3). Note that the crystallization of the system from below with the migrating false bottom increasing in thickness and the solidification of the system from above with a two-phase region caused by a decrease in the atmospheric temperature, can be completely independent. In other words, these two solidification mechanisms can occur in different times or seasons. As this takes place, the phase transition boundaries of the false bottom $a(t)$ and $b(t)$ are shown to move proportionally to the freezing time t (Alexandrov and Malygin, 2011; Alexandrov and Nizovtseva, 2008b), whereas two upper boundaries $h(t)$ and $c(t)$ grow as square root of time (Alexandrov and Malygin, 2011; Alexandrov et al., 2006, 2007, 2008). This implies that the rate of false bottom migration is nearly constant. This theoretical conclusion obtained by Alexandrov et al. (2006) agrees with laboratory and field observations (Hanson, 1965; Martin and Kauffman, 1974) and with the laws of motion of the phase transition boundaries $a(t) \sim b(t) \sim t$ and $h(t) \sim c(t) \sim \sqrt{t}$ representing the main principles of self-similar processes (Alexandrov and Malygin, 2006). However in most cases the atmospheric temperature as well as far-field temperature and salinity in the ocean depend on time due to weather changes and oceanic currents caused by storms. Such time-dependent fluctuations would lead to deviations from the constant growth rate of the false bottom boundaries and are discussed further in the next section (see also Figs. 4 and 5).

4 External influences on ice growth

Another interesting feature is that several time periods of pond drainage lead to the formation of several under-ice ponds and false bottoms. Two underwater ice sheets, one under another, were found at station “Charlie” as was reported by Hanson (1965). Stratigraphic measurements of different cores sampled during the ARCTIC 91 cruise analyzed by Eicken (Eicken, 1994) show that the evolution of the false bottom creates a columnar/granular ice structure, while an ice layer with a purely columnar structure characterizes pack ice on top of the meltwater (Fig. 3). Moreover, structural transitions from the columnar ice to the columnar/granular and granular ice were observed at different depths of ice core sampling sites, which are connected with the freezing process of under-ice melt ponds (Eicken, 1994). As a result, these transitions can be formed when the freezing process of all liquid layers completes. A theory for describing such a process of false bottom interaction with a moving layer of upper ice representing a mushy region has been developed for the first time by Alexandrov and Malygin (2011). Thus, many structural transitions in the ice column can be interpreted as a result of the interaction of phase transitions because migrating structures of the false bottom located below one another are found in nature. It should however be kept in mind that there are other plausible explanations for the alternation of columnar and granular ice in the pack ice cover, as discussed by Eicken (1994).

Since the heat and mass exchange at the false bottom/sea water boundary $y = b(t)$ is strongly influenced by the turbulent fluxes of heat $\langle w'T' \rangle_o$ and salt $\langle w'S' \rangle_o$ in the ocean as shown by McPhee and co-authors in numerous papers (McPhee, 1986, 1987, 1990; McPhee et al., 1999, 2008), the false bottom growth has to be controlled by physical parameters and conditions in the ocean. As discussed by McPhee in his monograph (McPhee, 2008), these turbulent fluxes are connected by means of the liquidus slope m as $\langle w'T' \rangle_o = -m \langle w'S' \rangle_o$. In simple words, this expression shows that turbulent heat is released from the sea water at just the rate required to maintain the sea water at its freezing temperature as salt is added at the false bottom/ocean boundary. Using dimensional analysis, McPhee (2008) represents these turbulent fluxes in terms of temperature and salinity differences between the false bottom/ocean boundary (temperature T_o, salinity S_o) and the deep ocean (temperature T_∞, salinity S_∞) quantities:

$$\langle w'T' \rangle_o = \alpha_\mathrm{h} u_* (T_\infty - T_o), \quad \langle w'S' \rangle_o = \alpha_\mathrm{s} u_* (S_\infty - S_o), \tag{1}$$

where u_* is the friction velocity (a measure of the turbulent velocity) estimated experimentally or calculated theoretically on the basis of the Rossby-number similarity analysis, and α_h and α_s are turbulent exchange coefficients for heat and salt determined experimentally. The ratio $35 \le \alpha_\mathrm{h}/\alpha_\mathrm{s} \le 70$ is the combination obtained by minimizing the root-mean square error between field observations and theoretical models (McPhee, 2008; McPhee et al., 2008, 1999).

As theoretically shown (Alexandrov and Malygin, 2011; Alexandrov and Nizovtseva, 2008a, b), the false bottoms may have a significant impact on the heat fluxes in the Arctic sea ice. For example, the heat flux $J(t) = \alpha_\mathrm{h}\rho_\mathrm{w}c_\mathrm{w}u_*(T_\infty - T_o)$, where ρ_w and c_w are the density and the specific heat of water, determined at the false bottom/ocean boundary and caused by its upward migration is of the order of the heat flux $J_\mathrm{at}(t)$ determined at the ice/atmosphere boundary (Fig. 4). The flux J is directed from the false bottom/ocean boundary into the ocean's depth (this direction corresponds to negative values of the flux), while boundary flux J_at has an opposite direction. The calculations based on original analytical approaches carried out by Alexandrov and co-authors (Alexandrov and Malygin, 2011; Alexandrov and Nizovtseva, 2008a, b), show that these fluxes are comparable in their order of magnitude. The heat flux J (after day 207 at the SHEBA site) changes its sign due to temporary turbulent conditions (e.g. storm) in the ocean (Fig. 4), which substantially increase the friction velocity. As a result, the salt flux from the ocean to the ice increases, and in its turn a rapid ablation of the false bottom occurs. An increase of the brine salinity reduces the phase transition temperature $T_o = -mS_o$ which becomes less than the ocean temperature T_∞. By this it is meant that the temperature difference $T_\infty - T_o$ becomes positive and the heat flux J changes its sign. In other words, as is shown in Fig. 4, the ocean–ice heat flux is directed toward the ocean during the quiescent period but toward the atmosphere during the storm. Note that the temperature and salinity distributions within the false bottom layer practically represent linear functions of the spatial coordinate at different times as is demonstrated in Fig. 4 in accordance with the theory developed by Alexandrov

Title Page
Abstract
Introduction
Conclusions
References
Tables
Figures
◄◄
►►
◄
►
Back
Close
Full Screen / Esc
Printer-friendly Version
Interactive Discussion

and Nizovtseva (2008b) for SHEBA data. The same linear profiles were observed in laboratory experiments carried out by Martin and Kauffman (1974).

Generally speaking, the false bottom's evolution can strongly change the resultant heat flux due to the appearance of the flux J being comparable with the other contributions to the resulting heat flux. So, for example, field experiments carried out by Perovich and Maykut (1990) show that the fluctuations of the latent heat flux caused by the seawater freezing in the ice cracks range from 8 to 40 $\mathrm{W\,m^{-2}}$. The measurements were made between 22 June and 10 July, i.e., in the period typical for the false bottom's formation. As this takes place, the ice–ocean heat flux can be directed upward or downward at different times, with an average value of $-12.9\,\mathrm{W\,m^{-2}}$ for AIDJEX (Arctic Ice Dynamics Joint Experiment) and $-5.6\,\mathrm{W\,m^{-2}}$ for SHEBA data. These estimates are calculated by Alexandrov and Nizovtseva (2008b) on the basis of their theoretical model of the false bottom represented as a mushy layer. Note that this flux is comparable with other contributions (heat fluxes) such as solar radiation divergence and the upward ocean heat flux from depth. Thus, the evolution of false bottoms can strongly influence the heat exchange between the ocean and atmosphere, which is especially pronounced in the spring–summer period, for which the growth of the second bottom is typical. Another important point is that the rate of the false bottom ice growth is nearly constant and the laws of motion of its phase transition layer are proportional to the process time as shown from theoretical approaches (Alexandrov and Nizovtseva, 2008a, b). The latter can be used to estimate the aerial false bottom ice dynamics within the time periods typical for its formation.

As amply discussed before (e.g. Shirasawa et al., 1997; McPhee et al., 2003; Uusikivi et al., 2006), the evolution of false bottoms in nature depends on real under-ice turbulent fluxes, which are essentially different in coastal seas and ocean areas during tidal and storm conditions. In order to demonstrate their influence on false bottom dynamics, we describe the real friction velocity fluctuations by means of stochastic methods (Fig. 5, details for the random fluctuations of the friction velocity by means of a stochastic differential equation with a standard Gaussian process are described by Alexandrov et al., 2013). The key result is that random fluctuations of the friction velocity, produced by turbulent motion in the ocean, substantially reduce the false bottom thickness in comparison with its deterministic growth (approximately 30 % reduction in the false bottom thickness after the 5 day growth). This reduction can be up to 10 cm for several days. This suggests that the ice freeze-on rate is essentially different in the case of quiescent and storm conditions.

Finally it should be noted that this freezing process from below occurs, in particular, under ice shelves, where fresh-water glacial run-off at a temperature very near 0 °C accumulates behind the ice shelf until the fresh water flows out beneath the shelf (where temperature is below zero, e.g. −1. 6 °C). Similarly, as was demonstrated by Lyons and co-authors (Lyons, 1971), the heat transfer between the salt and fresh water is responsible for 20 $\mathrm{cm\,yr^{-1}}$ ice growth under the Ward Hunt Ice Shelf maintaining the mass balance of approximately 100 $\mathrm{km^2}$ of the ice shelf. Thus, the evolution of false bottoms can strongly influence the heat exchange between the ocean and the atmosphere, which is especially pronounced in the spring-summer period, for which the growth of the second bottom is typical.

5 Conclusions

The evolution of false bottoms challenges certain aspects of our understanding of interactions between the ocean and atmosphere. A key question is how the false bottom development changes regional and large-scale properties of the overall ice pack? During the spring–summer time periods of thickening of false bottoms, a significant heat flux of the order of 10–100 $\mathrm{W\,m^{-2}}$ appears as a result of their growth and evolution. This heat flux (comparable to other heat fluxes such as solar radiation divergence and the upward ocean heat flux from depth) appears locally but will have global consequences for the heat budget. Therefore it is very important to measure the extent and aerial coverage of false bottoms in Arctic seas.

A second unanswered question is how the friction velocity and turbulent exchange coefficients influence the growth and subsequent decay/migration of a false bottom? The predicted false bottom dynamics is sensitive to the values chosen for u_*, α_h and α_s. All of them should be found in accordance with regional peculiarities of underwater ice growth, on the basis of detailed measurements of migration rates and heat fluxes and their comparisons with predicted theoretical estimates. Note that false bottoms break up in storms should also be taken into account to achieve a better parameterization of turbulent fluxes. Considering these processes should give us a more accurate modeling of sea-ice dynamics in the Arctic during summer.

As false bottoms represent the only source of ice accretion during the polar summer, one should also wonder about the regional balance between the thinning and shrinking of the sea ice cover due to its surface ablation and the thickening of ice due to the false-bottom evolution. The feature of underwater ice growth should also be kept in mind in the climate change studies, as together with general ice ablation, the false bottom ice growth represents a mechanism of its partial reproduction in the spring–summer seasons.

Lastly, as a counterpart of the above: what is the role of false bottoms on the surface albedo? On the one hand, the thickening of thin ice by false-bottom growth leads to smaller ice-free areas resulting in increased reflected radiation from the surface (albedo). On the other hand, the mechanism of false-bottom formation has a direct bearing on the initiation of surface melt ponds which decrease the ratio of reflected radiation from the surface to incident radiation upon it (albedo).

Supplementary material related to this article is available online at http://www.the-cryosphere-discuss.net/7/5659/2013/tcd-7-5659-2013-supplement.zip.

Acknowledgements. We acknowledge the support of Russian government under the contracts 11.G34.31.0064 and 14.A18.21.0858 of the Federal Target Program "Scientific and Academic – Teaching Staff of Innovative Russia" in 2009–2013.

References

Ackley, S. F.: A review of sea-ice weather relationships in the Southern Hemisphere in Sea Level, Ice and Climatic Change (IAHS Publication), Washington DC, 127–159, 1979.

Alexandrov, D. V. and Malygin, A. P.: Self-similar solidification of an alloy from a cooled boundary, Int. J. Heat Mass Trans., 49, 763–769, doi:10.1016/j.ijheatmasstransfer.2005.07.047, 2006.

Alexandrov, D. V. and Malygin, A. P.: Nonlinear dynamics of phase transitions during seawater freezing with false bottom formation, Oceanology, 51, 940–948, doi:10.1134/S0001437011060014, 2011.

Alexandrov, D. V. and Nizovtseva, I. G.: Nonlinear dynamics of the false bottom during seawater freezing, Dokl. Earth Sci., 419, 359–362, doi:10.1134/S1028334X08020384, 2008a.

Alexandrov, D. V. and Nizovtseva, I. G.: To the theory of underwater ice evolution, or nonlinear dynamics of "false bottoms", Int. J. Heat Mass Trans. 51, 5204–5208, doi:10.1016/j.ijheatmasstransfer.2007.11.061, 2008b.

Alexandrov, D. V., Malygin, A. P., and Alexandrova, I. V.: Solidification of leads: approximate solutions of non-linear problem, Ann. Glaciol., 44, 118–122, 2006.

Alexandrov, D. V., Aseev, D. L., Nizovtseva, I. G., Huang, H.-N., and Lee, D.: Nonlinear dynamics of directional solidification with a mushy layer. Analytic solutions of the problem, Int. J. Heat Mass Trans. 50, 3616–3623, 2007.

Alexandrov, D. V., Nizovtseva, I. G., Malygin, A. P., Huang, H.-N., and Lee, D.: Unidirectional solidification of binary melts from a cooled boundary: analytical solutions of a nonlinear diffusion-limited problem, J. Phys. Cond. Mat., 20, 114105, doi:10.1088/0953-8984/20/11/114105, 2008.

Alexandrov, D. V., Bashkirtseva, I. A., Malygin, A. P., and Ryashko, L. B.: Sea ice dynamics induced by external stochastic fluctuations, Pure Appl. Geophys., 170, 2273–2282, 2013.

Budikova, D.: Role of Arctic sea ice in global atmospheric circulation: a review, Global Planet. Change, 68, 149–163, doi:10.1016/j.gloplacha.2009.04.001, 2009.

Buyevich, Yu. A., Alexandrov, D. V., and Mansurov, V. V.: Macrokinetics of Crystallization, Begell House Inc., New York, 2001.

Cherepanov, N. V., Nazintsev, I. L., and Tyshko, K. P.: Contact supercooling of water layers and bottom ice formation in the sea in Electro Physical and Physical-Mechanical Properties of Ice, edited by: Bogordskii, V. V., Gavrilo, V. P., Gidrometeoizdat, St. Petersburg, 124–134, 1989.

Eicken, H.: Structure of under-ice melt ponds in the central Arctic and their effect on the sea-ice cover, Limnol. Oceanogr. 39, 682–694, 1994.

Eicken, H., Krouse, H. R., Kadko, D., and Perovich, D. K.: Tracer studies of pathways and rates of meltwater transport through Arctic summer sea ice, J. Geophys. Res. 107, 8046, doi:10.1029/2000JC000583, 2002.

Eicken, H., Gradinger, R., Gaylord, A., Mahoney, A., Rigor, I., and Melling, H.: Sediment transport by sea ice in the Chukchi and Beaufort seas: increasing importance due to changing ice conditions, Deep-Sea Res. II, 52, 3281–3302, doi:10.1016/j.dsr2.2005.10.006, 2005.

Gradinger, R.: Occurrence of an algal bloom under Arctic pack ice, Mar. Ecol.-Prog. Ser., 131, 301–305, 1996.

Hanson, A. M.: Studies of the mass balance of arctic pack ice floes, J. Glaciol. 5, 701–709, 1965.

Jeffries, M. O., Schwartz, K., Morris, K., Veazey, A. D., Krouse, H. R., and Gushing, S.: Evidence for platelet ice accretion in Arctic sea ice development, J. Geophys. Res. 100, 10905–10914, doi:10.1029/95JC00804, 1995.

Junge, K., Eicken, H., and Deming, J. W.: Bacterial activity at −2 to −20 °C in Arctic wintertime sea ice, Appl. Environ. Microbiol., 70, 550–557, doi:10.1128/AEM.70.1.550-557.2004, 2004.

Light, B., Eicken, H., Maykut, G. A., and Grenfell, T. C.: The effect of included participates on the spectral albedo of sea ice, J. Geophys. Res., 103, 27739–27752, doi:10.1029/98JC02587, 1998.

Lyons, J. B., Savin, S. M., and Tamburi, A. J.: Basement ice, Ward-Hunt Ice Shelf, Ellesmere Island, Canada, J. Glaciol. 10, 93–100, 1971.

Martin, S. and Kauffman, P.: The evolution of under-ice melt ponds, or double diffusion at the freezing point, J. Fluid Mech., 64, 507–527, 1974.

McPhee, M. G.: The upper ocean, in: The Geophysics of Sea Ice, edited by: Untersteiner, N., Plenum, New York, 133–141, 1986.

McPhee, M. G.: A time-dependent model for turbulent transfer in a stratified oceanic boundary layer under pack ice, J. Geophys. Res. 92, 6977–6986, 1987.

McPhee, M. G.: Small scale processes, in: Polar Oceanography, Part A: Physical Science, Academic, San Diego, Calif., 287–334, 1990.

McPhee, M. G.: Air–Ice–Ocean Interaction: Turbulent Boundary Layer Exchange Processes, Springer, New York, 2008.

McPhee, M. G., Kottmeier, C., and Morison, J. H.: Ocean heat flux in the central Weddell Sea in winter, J. Phys. Oceanogr. 29, 1166–1179, 1999.

McPhee, M. G., Kikuchi, T., Morison, J. H., and Stanton, T. P.: Ocean-to-ice heat flux in the North pole environmental observatory, Geophys. Res. Lett., 30, 2274, doi:10.1029/2003GL018580, 2003.

McPhee, M. G., Morison, J. H., and Nilsen, F.: Revisiting heat and salt exchange at the ice–ocean interface: ocean flux and modeling considerations, J. Geophys. Res., 113, C06014, doi:10.1029/2007JC004383, 2008.

Nansen, F.: Farthest North, Harper & Brothers, New York, 1897.

Notz, D., McPhee, M. G., Worster, M. G., Maykut, G. A., Schlünzen, K. H., and Eicken, H.: Impact of underwater-ice evolution on Arctic summer sea ice, J. Geophys. Res., 108, 3223, doi:10.1029/2001JC001173, 2003.

Peixoto, J. P. and Oort, A. H.: Physics of Climate, American Institute of Physics, New York, 1992.

Perovich, D. K. and Maykut, G. A.: Solar heating of a stratified ocean in the presence of a static ice cover, J. Geophys. Res., 95, 18233–18245, doi:10.1029/JC095iC10p18233, 1990.

1. Perovich, D. K., Andreas, E. L., Curry, J. A., Eiken, H., Fairall, C. W., Grenfell, T. C., Guest, P. S., Intrieri, J., Kadko, D., Lindsay, R. W., McPhee, M. G., Morison, J., Moritz, R. E., Paulson, C. A., Pegau, W. S., Persson, P. O. G., Pinkel, R., Richter-Menge, J. A., Stanton, T., Stern, H., Sturm, M., Tucker III, W. B., and Uttal, T.: Year on ice gives climate insights, Eos. Trans. AGU, 80, 485–486, doi:10.1029/EO080i041p00481-01, 1999.

Perovich, D. K., Grenfell, T. C., Richter-Menge, J. A., Light, B., Tucker III, W. B., and Eicken, H.: Thin and thinner: sea ice mass balance measurements during SHEBA, J. Geophys. Res., 108, 8050, doi:10.1029/2001JC001079, 2003.

Pfirman, S., Lange, M. A., Wollenburg, I., and Schlosser, P.: Sea ice characteristics and the role of sediment inclusions in deep-sea deposition: Arctic–Antarctic comparisons in Geological History of the Polar Oceans: Arctic versus Antarctic, edited by: Bleil, U. and Thiede, J., Kluwer, Netherlands, 187–211, 1990.

Polashenski, C., Perovich, D., Richter-Menge, J., and Elder, B.: Seasonal ice mass-balance buoys: adapting tools to the changing Arctic, Ann. Glaciol. 52, 18–26, 2011.

Randall, D., Curry, J., Battisti, D., Flato, G., Grumbine, R., Hakkinen, S., Martinson, D., Preller, R., Walsh, J., and Weatherly J. W.: Status of and outlook for large-scale modelling of atmosphere ice–ocean interactions in the Arctic, B. Am. Meteorol. Soc., 79, 197–219, 1998.

Shirasawa, K., Ingram, R. G., and Hudier, E. J. J.: Oceanic heat fluxes under thin sea ice, Saroma-ko Lagoon, Hokkaido, Japan, J. Mar. Syst., 11, 9–19, 1997.

Spindler, M.: A comparison of Arctic and Antarctic sea ice and the effects of different properties on sea ice biota, in: Geological History of the Polar Oceans: Arctic versus Antarctic, edited by: Bleil, U. and Thiede, J., Kluwer, Netherlands, 173–186, 1990.

Steele, M., Mellor, G. L., and McPhee, M. G.: Role of the molecular sublayer in the melting or freezing of sea ice, J. Phys. Oceanogr. 19, 139–147, 1989.

Stefan, J.: Über einige probleme der theorie der wärmeleitung. Sitzungsberichte de Mathematisch-Naturawissenschaftlichen Classe der Kaiserlichen, Akademie der Wissenschaften, 98, 473–484, 1889.

The LeadEx Group (1993): The lead experiment, Eos. Trans. AGU, 74, 393–397, doi:10.1029/93EO00341, 1993.

Untersteiner, N. and Badgley, F. I.: Preliminary results of thermal budget studies on Arctic pack ice during summer and autumn. in Arctic Sea Ice, Natl. Acad. of Sci., Natl. Res. Counc., Washington DC, 85–92, 1958.

Uusikivi, J., Ehn, J., and Granskog, M. A.: Direct measurements of turbulent momentum, heat and salt fluxes under landfast ice in the Baltic Sea, Ann. Glaciol. 44, 42–46, 2006.

Wadhams, P.: The underside of sea ice imaged by side-scan sonar, Nature, 333, 161–164, 1988.

Wadhams, P. and Martin, S.: Processes determining the bottom topography of multi-year Arctic sea ice, in: Sea Ice Properties and Processes, edited by: Weeks, W. F. and Ackley, S. F., Cold Regions Res. and Eng. Lab., Hanover, 136–141, 1990.

Weeks, W. F.: On Sea Ice, University of Alaska Press, Fairbanks, 2010.

Zubov, N.: Arctic Ice, US Navy Electronics Laboratory, San Diego, 1945.

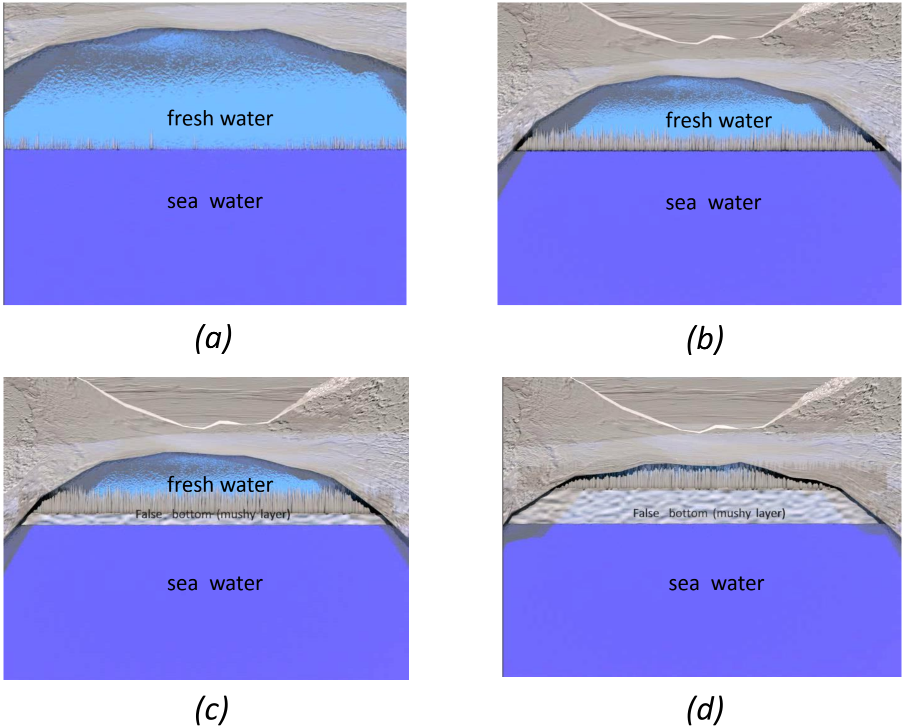

Fig. 1. The false bottom growth scheme animation screenshots (see also the Supplement).

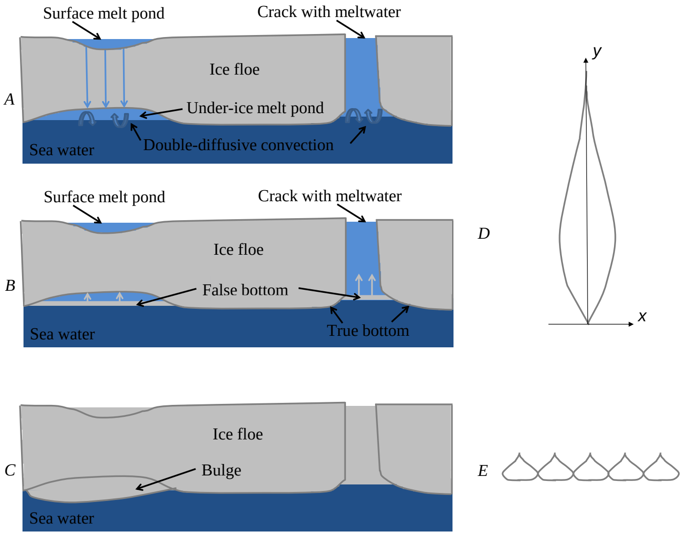

Fig. 2. A scheme of the false bottom formation drawn from Martin and Kauffman (1974) and Notz et al. (2003). **(A)** In the spring–summer time period, surface melt ponds, filled with low salinity meltwater, appear at the atmosphere–ice interface. This meltwater also collects in ice cracks above sea water level. Penetration of surface meltwater through the highly permeable ice matrix leads to the formation of under-ice melt ponds. Double-diffusive convection of heat and salt between this fresh (light) water and underlying salt (dense) water is responsible for the formation of false bottoms (panels **A** and **B**), **(B)** false bottoms grow upward sealing the under-ice pond from below, **(C)** the bottom and surface ponds as well as the water columns in cracks are completely frozen (winter). A slight bulge can be formed due to pressure build-up during the false bottom migration, **(D)** the crystal profile nucleated at the freshwater–seawater interface shown in accordance with the laboratory experiments and theoretical considerations presented by Martin and Kauffman (1974), **(E)** the ice sheet of growing crystals forming a false bottom (only schematic, not drawn to scale). A leveling mechanism of the under-ice topography is caused by the bottom ablation.

Title Page
Abstract
Introduction
Conclusions
References
Tables
Figures
|◀
▶|
◀
▶
Back
Close
Full Screen / Esc
Printer-friendly Version
Interactive Discussion

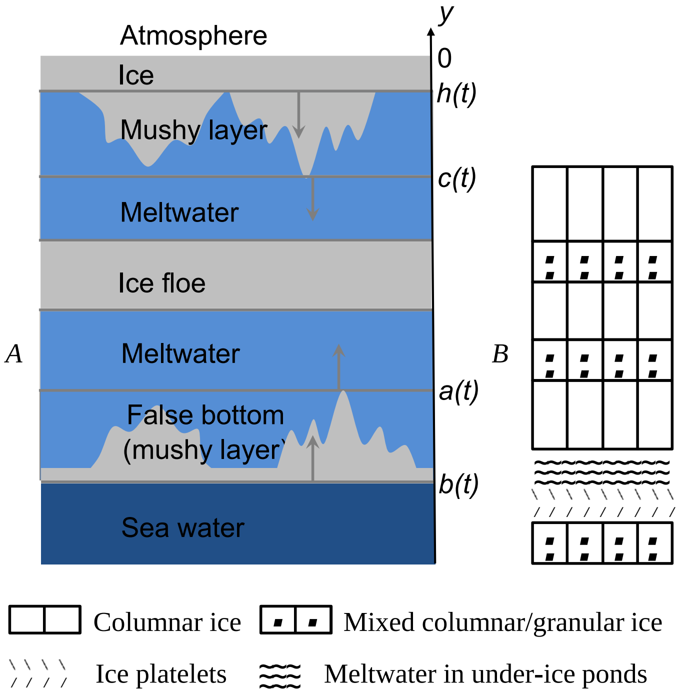

Fig. 3. "Pre-existing pack ice floe". **(A)** A scheme of possible directions of crystallization processes: (1) with the false bottom in the upward direction from the underwater melt pond to the atmosphere and (2) with freezing of the ice layer representing a two-phase (or mushy) region in the downward direction from the surface melt pond to the ocean, **(B)** schematic structures of the sea ice solidified with false bottoms (Eicken, 1994).

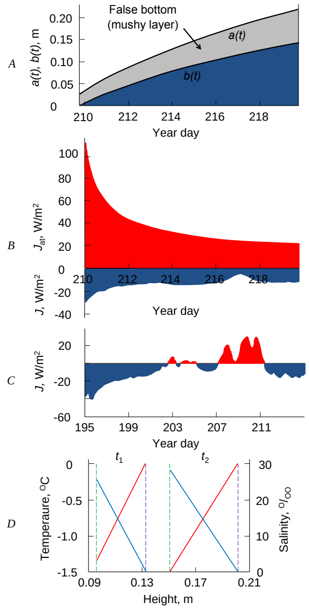

Fig. 4. The false bottom boundaries and fluxes drawn from Alexandrov and Nizovtseva, (2008b) and Alexandrov and Malygin (2011). **(A)** Evolution of the false bottom boundaries during AIJEX calculated on the basis of the false bottom theory (Perovich et al., 2003), **(B)** the heat fluxes $J(t)$ (at the false bottom/ocean boundary) and $J_{\text{at}}(t)$ (at the atmosphere/ice boundary) vs. the time based on the AIDJEX experiment (Perovich et al., 2003), **(C)** the heat flux $J(t)$ (at the false bottom/ocean boundary) vs. the time based on the SHEBA experiment (Alexandrov and Nizovtseva, 2008a, b), **(D)** the temperature (red lines) and salinity (blue lines) distributions in the false bottom based on the SHEBA experiment and calculated in accordance with the theory developed by Alexandrov and Nizovtseva (2008b). Two boundaries a (purple line) and b (green line) are shown at different times $t_2 > t_1$ (t_2 and t_1 correspond to 200 and 205 days of the year).

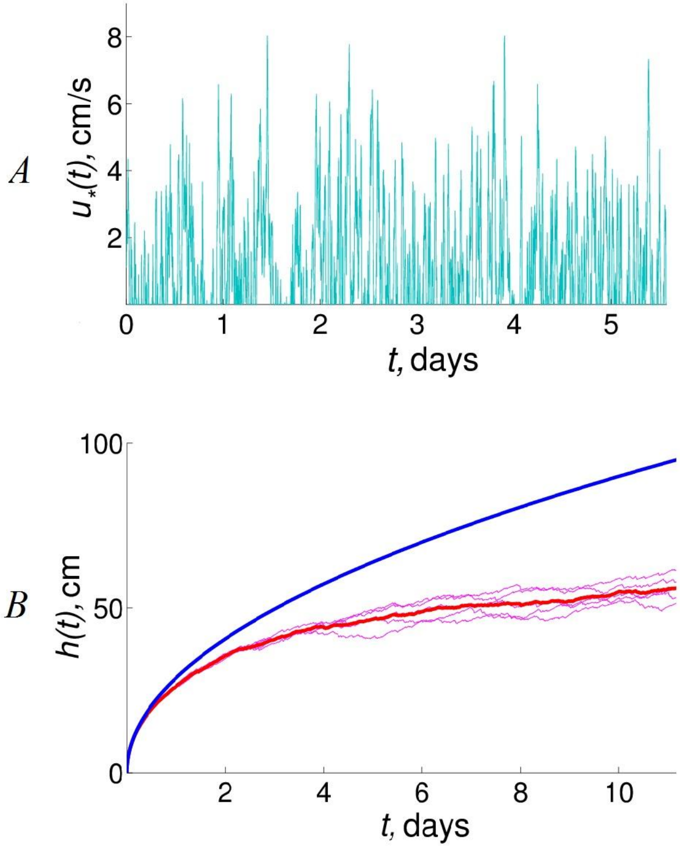

Fig. 5. (A) A sample path of the friction velocity with the mean value $\langle u_*(t) \rangle = 1.2\,\mathrm{cm\,s^{-1}}$, **(B)** sample paths of the false bottom thickness ($h(t) = a(t) - b(t)$, pink lines) and its mean value (red line) in the case of stochastic oscillations of the friction velocity (Alexandrov et al., 2013). The blue line represents the deterministic false bottom thickness in the absence of stochastic fluctuations.